Electrochemical approach to the dynamics of molecular recognition of redox enzyme sites by artificial cosubstrates in solution and in integrated systems

Nathalie Anicet,[a] Agnès Anne,[a] Christian Bourdillon,[b] Christophe Demaille,[a] Jacques Moiroux*[a] and Jean-Michel Savéant[a]

[a] *Laboratoire d'Electrochimie Moléculaire, Unité Mixte de Recherche Université–CNRS No 7591, Université de Paris 7–Denis Diderot, 2 place Jussieu, 75251 Paris Cedex 05, France*

[b] *Laboratoire de Technologie Enzymatique, UPRES-A No 6022, Université de Technologie de Compiègne, BP 20529, 60205 Compiègne Cedex, France*

Received 21st February 2000
First published as an Advance Article on the web 31st May 2000

Application of antigen–antibody technology allows the attachment to an electrode surface of an enzyme monolayer structure to which both the enzyme and the mediator are bound. As illustrated with the example of glucose oxidase and a ferrocene mediator, the enzyme preserves its full activity in such structures, which may be easily reproduced. In spite of their fixation to the structure, the mobility of the ferrocene heads is sufficient to ensure that its transport to the enzyme prosthetic group is not rate determining. The reaction is rather controlled by the prior formation of a complex between the ferrocenium ion and the flavin required for electron transfer to occur. The efficiency of this step is affected by steric hindrance and the various observations made with free-moving and attached ferrocene-ended poly(ethylene glycol) chains may be rationalized by the interplay of factors controlling their distribution and shape. Analyzing the dynamics of this system, in comparison with previous systems, was thus an occasion to shed further light on the recognition phenomenon. The enzyme monolayer integrated system is a good starting point for the step-by-step construction of spatially ordered multilayered assemblies with strong catalytic efficiencies. Fast responding systems are expected both in terms of electron transport and electron transfer between the mediator and the enzyme. The spatial order resulting from the step-by-step construction should allow a much more precise analysis of electron transport and electron transfer than in conventional assemblies of redox centers. Mastering both the construction and the functioning of such systems should help the design of more complex systems, integrating additional functionalities electrically controlled by means of their electron transport/electron transfer connection to the electrode surface.

Connecting an electrode with a redox enzyme allows the translation of specific chemical events taking place at the prosthetic group into easy-to-use electric signals or, conversely, to trigger and control enzymatic reactions by easy-to-manipulate potential and current variables. Applications may concern biosensors and preparative-scale transformations.[1–6] In most cases, direct electron

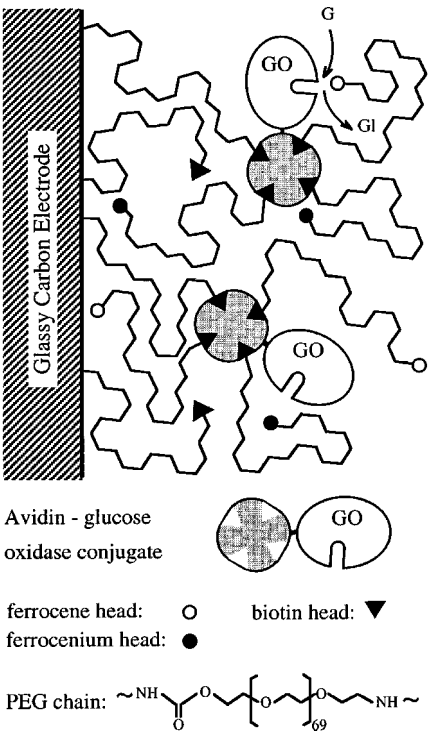

Scheme 1

transfer is prevented by the fact that the distance between the electrode and the prosthetic group is exceedingly large, by improper orientation of the adsorbed enzyme or by adsorptive denaturation. A redox mediator able to shuttle electrons between the electrode and the prosthetic group is then required. The mediator thus serves as a co-substrate to the enzyme replacing the natural co-substrate. Setting the electrode potential at a value appropriate for generating the active form of the mediator from its passive form thus results in an enhancement of the current, which is a measure of the catalysis of the electrochemical oxidation (or reduction) of the substrate by the mediator–enzyme system. Treatments available from other types of catalysis (redox and chemical) of electrochemical reactions may thus be adapted for extracting the kinetic information from the catalytic current responses.[7–9] Attachment of the enzymatic catalytic systems to the electrode has obvious advantages for biosensor and synthesis applications. For this purpose, "wiring" of enzymes to electrodes by entrapment in gels or polymers is well documented.[10–12] Imitation of natural systems has inspired a quest for more precisely organized systems based on the docking properties of proteins.[13–15] Several modes of linking between such molecular architectures and electrodes have been investigated. One involves electrostatic interactions[16–18] and the two others are antigen–antibody[19–23] and avidin–biotin[24–30] binding.

The latter two technologies have been applied to the deposition of monomolecular layers on electrode surfaces[19,29] as well as to the step-by-step construction of spatially ordered multilayered coatings[20,21,28,30] in which the enzyme activity has not been deteriorated by the attachment procedure. It is noteworthy that the construction of multilayered systems is more difficult with the avidin–biotin technology than with the antigen–antibody technology owing to the reversibility of the binding in the former case.[28] All these systems lend themselves to a quantitative cyclic voltammetric analysis of their dynamics. It is thus possible, as demonstrated with the example of the oxidation of glucose by glucose oxidase, to fully characterize the kinetics of the enzymatic reaction and of the electron transfer reaction between the artificial mediator and the enzyme in these immobilized systems and to compare them with the values found in homogeneous solution.

Most of these studies have been performed in cases where the mediator is homogeneously dispersed in the solution. There is a need for more integrated systems in which the electron carrier

would be attached to the structure in a spatially defined manner and which would lend themselves to a full kinetic characterization. One such monomolecular layer system using avidin–biotin technology (Scheme 1) has been previously described.[29] However, because of the aforementioned difficulties, this system does not provide an easy starting point for the construction of integrated multi-monomolecular layer coatings. This is why we attempted the synthesis of an integrated monolayer coating based on antigen–antibody binding in which the electron transfer mediator is attached to the supramolecular structure. This system, depicted below, also possesses the advantage of having a larger number of mediator molecules attached to the monolayer than in the avidin–biotin system depicted in Scheme 1, thus giving rise to higher and more easily measurable currents. Determination of the rate constants of the key steps (glucose half-reaction and electron transfer between the mediator and the enzyme) will be an occasion to pursue the discussion of molecular recognition effects initiated with other systems.

Construction of an antigen–antibody based integrated monolayer

As sketched in Scheme 2, the construction of the antigen–antibody enzyme monolayer in which both the enzyme and the mediator are attached starts with the adsorption onto the glassy carbon electrode of an antibody produced in goat.[19,22] In a second step, it serves as an antigen which is recognized by an anti-goat antibody produced in mouse, previously labeled with poly(ethylene glycol) (PEG) chains terminated by a ferrocene head (designated PEGFc). The synthesis of these chains, which contain an average of 76 $O–CH_2–CH_2$ units was as described in refs. 31 and 32 and the procedure for grafting the PEGFc chains onto the anti-goat antibody was as in ref. 32 where it

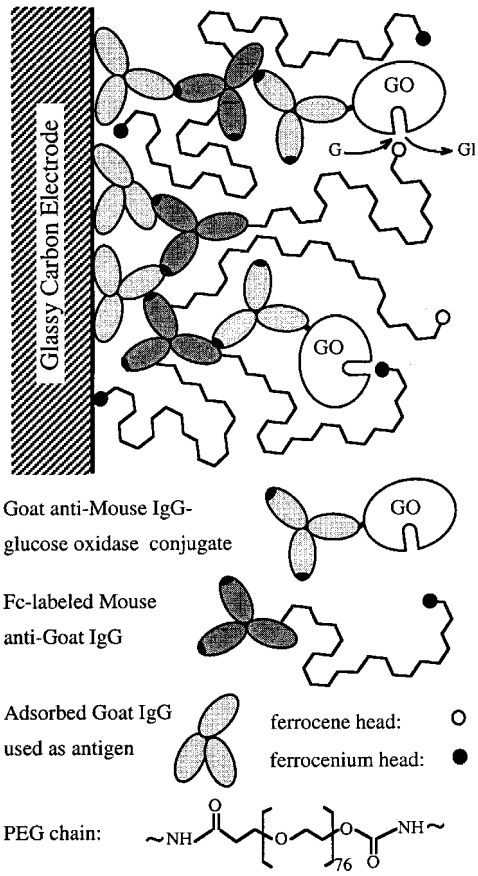

Scheme 2

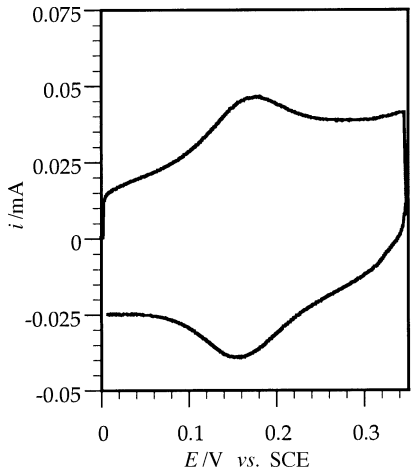

Fig. 1 Reversible surface wave of the ferrocene heads in the system depicted in Scheme 2 in the absence of glucose at a 0.07 cm^2 glassy carbon in a pH 8.0 phosphate buffer (0.1 M ionic strength). Scan rate: 0.02 V s^{-1}. Temperature = 25 °C.

has been shown that each antibody bears an average of 17 PEGFc chains. A third layer containing the enzyme is finally grafted onto the second layer, exploiting the recognition of the mouse IgG immobilized in the second monolayer by the anti-mouse glucose oxidase conjugate. The amount of PEGFc chains thus grafted may be derived from the cyclic voltammetry of the system in the absence of glucose (Fig. 1) by integration of the faradaic current obtained after subtraction of the background current (a steady value is reached after 48 h equilibration). The surface concentration thus found is $\Gamma_P^0 = 1.2 \pm 0.2 \times 10^{-11}$ mol cm^{-2}, corresponding to a surface concentration of $0.7 \pm 0.1 \times 10^{-12}$ mol cm^{-2} of PEGFc labeled antibodies.

When glucose is added to the solution, the cyclic voltammetric wave loses its reversibility, increases in height and takes a characteristic plateau shape reflecting the enzymatic catalysis of glucose oxidation with bound ferrocene acting as co-substrate. The kinetics of the reaction are analyzed in detail below.

If, in addition to glucose, ferrocene methanol is added to the solution, a much larger cyclic voltammetric catalytic response is obtained. The contribution of the mediation by PEGFc to the catalytic current is then actually negligible compared to that of the mediation by the solution of ferrocene methanol (0.4 mM). The amount of immobilized enzyme may be derived from the catalytic current obtained under these conditions,[19–22] leading to a surface concentration of $\Gamma_E^0 = 1.8 \pm 0.2 \times 10^{-12}$ mol cm^{-2}.

We note that the rate of recognition of the mouse IgG by the glucose oxidase anti-mouse conjugate is decreased by the presence of the PEGc chains. Indeed the coverage reaches a steady value only after 48 h. We also note that the surface concentrations of ferrocene mediator that can be measured before and after grafting of the anti-mouse glucose oxidase conjugate are practically the same, indicating that the PEG chains are not trapped within the assembly of immunoproteins, thus confirming the low compacity and penetrability of the whole structure.[19–22]

In the integrated system thus obtained, which contains both the enzyme and the mediator, the relative size of the various components are *ca.* those represented in Scheme 1. At full extension, the PEGFc chains are about 250 Å long, on average, while the diameter of each of the immunoglobulins and of glucose oxidase is *ca.* 90 Å.

Dynamics of the integrated system

Typical catalytic cyclic voltammograms obtained in the presence of glucose (the bulk concentration: C_G^0) are shown in Fig. 2. They are plateau-shaped and independent of the scan rate when the scan rate is lower than 0.02 V s^{-1}. The reactions taking place within the integrated system are

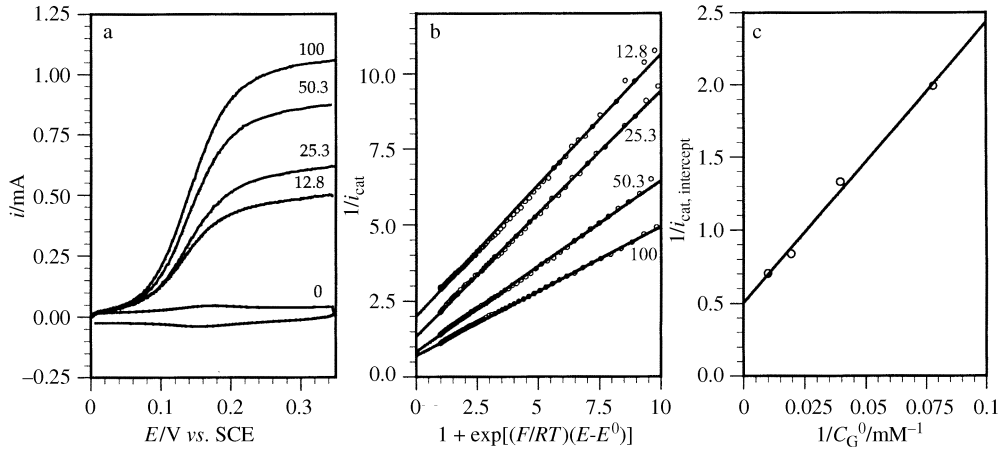

Fig. 2 Catalysis of glucose oxidation by the integrated system depicted in Scheme 2 as a function of glucose concentration (same conditions as in Fig. 1). (a) Cyclic voltammograms; (b) primary plots obtained along the wave (see text); (c) secondary plot. The numbers on the curves in (a) and (b) are the glucose concentrations in mM.

summarized in Scheme 3. At pH 8, at which all the experiments were carried out, the reduced enzyme exists under its deprotonated form, $FADH^-$.[22]

As shown earlier,[22] when the reduced form P of the mediator is introduced in solution, the oxidized form Q being generated at the electrode, the current measured in the presence of glucose results from the sum of the flux of Q toward the bulk and the flux of Q consumed by the enzyme catalyzed oxidation of glucose which takes place practically at the electrode surface. Along the whole wave we define the catalytic current, i_{cat}, as the difference between the currents in the presence and absence of glucose and i_{cat} is given by eqn. (1).[22]

$$\frac{1}{i_{cat}} = \frac{1}{2FSk\Gamma_E C_Q} + \frac{1}{2FS\Gamma_E}\left(\frac{1}{k_2} + \frac{1}{k_{red}\, C_G^0}\right) \quad (1)$$

where $k_{red} = k_1k_2/(k_{-1} + k_2)$, Γ_E is the surface concentration of the active enzyme FAD and C_Q is the volume concentration of the oxidized form of the mediator at the enzyme catalytic site.

In the integrated system, the displacement of the ferrocene heads of the terminally attached PEGFc chains is restricted to the length of the fully extended PEG chain. Then, if the concentrations of P and Q at the electrode surface obey the Nernst law and if both the rate of the enzyme-catalyzed reaction and the scan rate are slow enough to ensure that bounded diffusion of P and Q within the system is not rate controlling,[32] the overall kinetics are governed by the enzyme-catalyzed reaction. Under such conditions, the total current is the sum of the current required to generate a concentration of Q at the location of the enzyme site in equilibrium with the electrode potential and the current resulting from the consumption of Q by the enzyme-catalyzed reaction. Thus the catalytic current, still defined as the difference between the currents recorded in the presence and in the absence of glucose at any potential along the cyclic voltammogram, is given by eqn. (1).

$$FAD + G \underset{k_{-1}}{\overset{k_1}{\rightleftharpoons}} FADG$$

$$FADG \xrightarrow{k_2} FADH_2 + Gl$$

$$FADH_2 + 2\,Q \xrightarrow{k} FAD + 2\,P$$

Scheme 3

As seen in Fig. 1, the oxidation of the ferrocene heads and the reduction of the resulting ferrocenium molecules at the electrode are fast. They consequently obey Nernst's law, thus leading to eqn. (2) for the expression of C_Q.

$$C_Q = \frac{C_P^{es}}{1 + \exp[(F/RT)(E - E_{PQ}^0)]} \quad (2)$$

where E_{PQ}^0 is the standard potential of the mediator couple and C_P^{es} the total volume concentration of all forms of the mediator at the enzyme catalytic site. We will derive later on an expression of C_P^{es}. For the moment, we may check that the reciprocal of the current i_{cat} is a linear function of $1 + \exp[(F/RT)(E - E_{PQ}^0)]$, according to what is predicted by eqns. (1) and (2). That this is indeed the case for each glucose concentration can be seen in Fig. 2(b). We note, however, that the slope of these primary plots diminishes upon increasing glucose concentration, which is not expected since the rate constant k should be independent of this factor according to the mechanism sketched in Scheme 3. At low glucose concentration the slope is independent of this factor and corresponds to $kC_P^{es} = 47.5\ s^{-1}$, while at a glucose concentration of 100 mM, $kC_P^{es} = 97\ s^{-1}$. That this effect is related to the H-bonding interactions between glucose and the PEG chains is demonstrated by the fact that adding sucrose to a solution results in a decrease of the slope. If sucrose is added so as to keep the sucrose + glucose concentration constant and equal to the largest glucose concentration (100 mM), all the slopes become the same and equal to the value obtained at the largest glucose concentration, thus leading to a uniform value of k.

The intercepts in Fig. 2(b) are independent of the addition of sucrose and plotting them against $1/C_G^0$ leads to the secondary plot shown in Fig. 2(c). According to eqn. (1), the rate constants k_2 and k_{red} may be derived from the intercept and slope of the secondary plot respectively. We thus obtained $k_2 = 80 \pm 20\ s^{-1}$ and $k_{red} = 2.2 \pm 0.3 \times 10^3\ M^{-1}\ s^{-1}$ compared with the values found in solution[22,33] and in immobilized systems[22] in the absence of PEG of $700 \pm 100\ s^{-1}$ and $1.0 \pm 0.1 \times 10^4\ M^{-1}\ s^{-1}$ respectively. There is thus a slight but significant decrease of both rate constants. PEG does not interact strongly with proteins. Rather, it interacts with water, thus perturbing the protein–water structure.[34–37] It is not surprising that such perturbations may result in a decrease of the enzymatic activity.

Derivation of the rate constant k from the slope of the secondary plot rests on the estimation of C_P^{es}, the average of the total volume concentration of all forms of the mediator at the enzyme catalytic site. We may estimate the value of this concentration as follows.

Taking as origin the average plane where the PEGFc chains are anchored, the total volume concentration of the mediator heads, C_P^0, may be derived from a Gaussian distribution around the average anchoring plane according to eqn. (3),[32]

$$C_P^0(x) = \frac{\Gamma_P^0}{\sqrt{\pi}} \sqrt{\frac{\chi_{spr}}{2RT}} \exp\left(-\frac{\chi_{spr}\, x^2}{2RT}\right) \quad (3)$$

where x is the distance from the anchoring plane and χ_{spr} the force constant of the spring equivalent to the PEG chain. As shown earlier,[32] $\chi_{spr} l^2 = 8.65 \times 10^3\ J\ mol^{-1}$ and $l = 90$ Å, 1 l being the diameter of a sphere equivalent to a protein with a molecular weight of 150 000). Fig. 3 displays the concentration profile obtained from eqn. (3). The average plane where the glucose oxidase flavin centers are located is found between $1.5l$ (135 Å) and $2.5l$ (225 Å) from the average PEGFc anchoring plane (see Scheme 2). We see from Fig. 3(a), and in the blown-up representation in Fig. 3(b), that, in the region where the flavin centers are located, C_P^0 is very much smaller than its value for $x = 0$. Integration of the concentration profile in Fig. 3(b) leads to the average concentration in the region of interest (eqn. (4)),

$$\tilde{C}_P^{es} = \frac{\Gamma_P^0}{2l}\left[\mathrm{erf}\left(2.5l\sqrt{\frac{\chi_{spr}}{2RT}}\right) - \mathrm{erf}\left(1.5l\sqrt{\frac{\chi_{spr}}{2RT}}\right)\right] \quad (4)$$

thus leading to $\tilde{C}_P^{es} = 3.2 \times 10^{-5}$ M and therefore to $k = 1.5 \pm 0.3 \times 10^6\ M^{-1}\ s^{-1}$, erf being the error function.

It is interesting to compare the value of k thus found with the values characterizing systems where the enzyme is dispersed in the solution and where the cosubstrate is present either as free

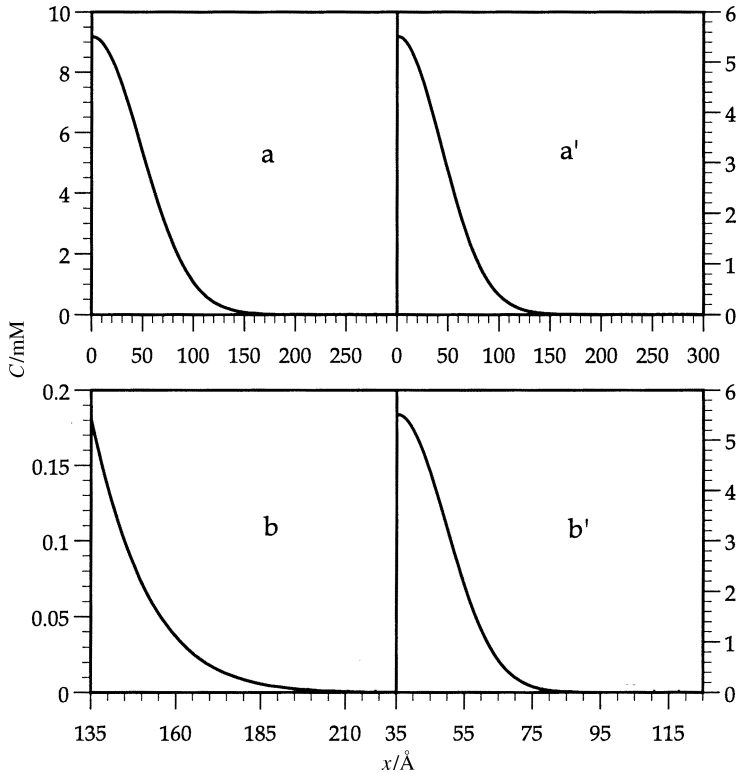

Fig. 3 Gaussian distribution of the ferrocene heads in the systems of Scheme 2 (a, b) and Scheme 1 (a′, b′). $\Gamma_P^0 = 1.2 \pm 0.2 \times 10^{-11}$ mol cm^{-2} (a, b), $= 6 \pm 3 \times 10^{-12}$ mol cm^{-2} (a′, b′).

PEGFc or a mixture of ferrocene methanol and PEG chains bearing no ferrocene heads. In this case, a catalytic plateau current i_{pl} is always obtained at positive enough potentials and:[22,38]

$$i_{pl} = FSD_{sol} C_P^0 \sqrt{2kC_E^0} \left\{ \frac{2}{\sigma} \left[1 - \frac{1}{\sigma} \ln(1+\sigma) \right] \right\}^{1/2}$$

with C_P^0 and C_E^0 the mediator and the enzyme bulk concentrations respectively, D_{sol} the diffusion coefficient of the mediator in solution and $\sigma = kC_P^0[(1/k_2) + (1/k_{red}C_G^0)]$. A pseudo-first order behavior, depicted by eqn. (5) is expected

$$i_{pl} = FSD_{sol} C_P^0 \sqrt{2kC_E^0} \tag{5}$$

for high glucose concentrations and low mediators. These conditions are fulfilled for $C_G^0 \geqslant 40$ mM and $C_G^0 \leqslant 4$ μM, in the second case and for $C_G^0 \geqslant 40$ mM and $C_P^0 \leqslant 20$ μM in the first. Application of eqn. (4) thus leads to $k = 2.2 \pm 0.2 \times 10^5$ M^{-1} s^{-1} in the first case and to $k = 1.2 \pm 0.2 \times 10^7$ M^{-1} s^{-1}. The latter result shows that the presence of PEG chains in the solution has practically no effect on the rate constant of the reaction between the soluble mediator, ferrocene methanol, and the prosthetic group of the enzyme.

Molecular recognition between glucose oxidase and one-electron artificial co-substrates

Before integrating the above data in the general discussion of the nature and extent of molecular recognition between glucose oxidase and one-electron artificial cosubstrates, let us recall previous results in this area. The first observations concerning this problem were made when investigating the reaction between glucose oxidase and three differently substituted ferrocenium ions in solution

as a function of pH. S-shape curves were obtained (see Fig. 8 in ref. 38), indicating that the reaction follows the mechanism depicted in Scheme 4, which also shows the values of the pK_as and standard potentials of interest. The thermodynamics and kinetics of the reaction of glucose oxidase with three ferrocenium ions are summarized in Table 1.

After checking that the protonation/deprotonation p1 and p3 are constantly at equilibrium in the pH region of interest, the overall, pH-dependent, rate constant k may be expressed by eqn. (6).

$$\frac{1}{k} = \frac{1 + (K_{p1}/[H^+])}{k_{e1} + (K_{p1}/[H^+])k_{e2}} + \frac{1 + (K_{p3}/[H^+])}{k_{e3} + (K_{p3}/[H^+])k_{e4}} \quad (6)$$

Applying eqn. (5) to the experimental data leads to two constants that characterize $FADH_2$, k_{ac} and $FADH^-$, k_{bas}, respectively, defined by eqns. (7), whose values are listed in Table 1.

$$\frac{1}{k_{ac}} = \frac{1}{k_{e1}} + \frac{1}{k_{e3}}; \qquad \frac{1}{k_{bas}} = \frac{1}{k_{e2}} + \frac{1}{k_{e4}} \quad (7)$$

In other words, both in acidic and basic media, the reaction is governed by the slower of the two successive electron transfer steps (see Scheme 4). If their rate constants are about the same, the overall rate constant is about half the average.

Perusal of Table 1 shows that the electron transfer steps between the ferrocenium ion and the reduced flavins are not the rate-determining steps. A first clue in this direction is that there is no correlation of the Marcus type between the rate constant and the driving force of the reaction as expected in outer-sphere electron transfer chemistry. For example, in the case of ferrocene carboxylate, the rate constant is only four times larger when going from acidic to basic media while a strong acceleration would be expected in view of the large increase in driving force (260 meV). Also, in basic medium, ferrocene methanol reacts faster than ferrocene carboxylate, against the order of the respective driving forces. Intrinsic barriers for electron transfer to the flavins should be small since electrons may be delocalized over the whole molecule. One would thus expect the rate constants to be close to the diffusion limit, at least in the cases in the thermodynamically most favorable cases. In fact, the rate constants are much below the diffusion limit ($k_{dif} = 5 \times 10^8$ M^{-1} s^{-1}) showing that electron transfer and diffusion are unlikely to govern the kinetics of the reac-

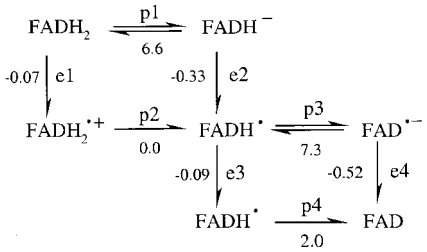

Scheme 4 The vertical arrows represents electron transfer steps and the attached numbers the corresponding standard potentials (in V *vs.* SCE).

Table 1 Thermodynamic and kinetics of the reaction of glucose oxidase was one-electron artificial cosubstrates in solution[a]

	Ferrocene methanol		Ferrocene carboxylate		(Dimethylamino) methylferrocene	
Acid medium	e1	e3	e1	e3	e1	e3
$\Delta G^{0\,b}$	−0.26	−0.28	−0.36	−0.38	−0.44	−0.46
Log k_{ac}/M^{-1} s^{-1}	4.8		4.7		5.4	
Basic medium	e2	e4	e2	e4	e2	e4
$\Delta G^{0\,b}$	−0.52	−0.71	−0.62	−0.81	−0.70	−0.89
Log k_{bas}/M^{-1} s^{-1}	7.1		5.3		7.4	

[a] From refs. 38 and 39. [b] Standard free enthalpy of the reaction in eV.

tion. These observations suggest that the rate-determining step is the formation of a precursor complex between the co-substrate and the flavin, entrenched in the protein structure, and possessing the geometrical characteristics appropriate for the electron transfer to occur.[40,41] This picture is confirmed by the effect of electrostatic attraction helping the formation of the precursor complex as demonstrated by the fact that, with the positively charged ferrocenium methanol and (dimethylamino)methylferrocenium, the reaction is two orders of magnitude faster in basic medium than in acidic medium whereas the rate constants are about the same with the uncharged ferrocenium carboxylate.

These data thus point to the existence of a certain degree of molecular recognition between glucose oxidase and artificial one-electron co-substrates in the ferrocenium series. Specificity of these interactions seemed to receive a spectacular confirmation when chiroselective electron transfer from glucose oxidase to a ferrocenium ion (from *N*,*N*-dimethyl-1-ferrocenylethylamine) was reported.[42] It was, however, shown later on that the catalytic responses of the two enantiomers are the same within experimental uncertainty pointing to the conclusion that molecular recognition of ferrocenium co-substrates by oxidase is not precise enough to lead to chiroselective electron transfer. Recognition is required for electron transfer to occur and the imperfect matching between the artificial co-substrate and glucose oxidase slows down electron transfer, thus offering some resistance against a largely favorable driving force. However, the resistance is not very efficient, resulting in large rate constants, making ferrocenium ions quite efficient co-substrates to glucose oxidase.

It is noteworthy that the rate constants of the reaction of ferrocene methanol with glucose oxidase remain the same when the enzyme is attached to an antibody bound to an antigen itself irreversibly adsorbed onto the electrode surface.[19] The same is true with multilayer system obtained by successive deposition of monolayers by the same technique.[20,21]

Gathering data obtained in this work and in previous investigations, Table 2 summarizes values of the rate constant of the reaction of glucose oxidase with ferrocenium ions obtained in basic solution in various systems where the formation of the precursor complex may be more or less sterically hampered.

A first remark is that the presence of the PEG chains in the solution does not influence appreciably the rate of the reaction of ferrocenium methanol with glucose oxidase when they are both present in the solution. The decrease of the rate constant when going to PEGFc chains of the type shown in Scheme 2 dispersed in the solution is therefore due to another cause than an interaction of the enzyme with poly(ethylene glycol) chains. It is unlikely that it is caused by an inductive substituent effect. The standard potential of PEGFc heads is 0.16 V *vs.* SCE *vs.* 0.19 for ferrocene methanol. We have seen that the rate constants are almost insensitive to the driving force, provided it is large. Such a small change in driving force thus has a negligible effect on the value of the rate constant. A likely explanation of the observed effect is as follows. PEGFc chains are random coils[43] occupying a spheric volume of approximately 40 to 50 Å diameter.[31] In a large fraction of the very many conformations of the chains, the ferrocenium head is deeply embedded in the coil, thus rendering the formation of the precursor complex difficult and, hence, the reaction is slower.

Coming to the case where the PEGFc chains are attached as depicted in Scheme 2, we note (Table 2) that the rate constant is smaller than with ferrocene methanol but larger than with PEGFc chains freely moving in the solution. A first remark in this respect is that the bounded

Table 2 Rates constants of the reaction between glucose oxidase and ferrocenium ions[a]

System	$k/M^{-1}\ s^{-1}$
Glucose oxidase in solution, ferrocene methanol in solution	1.2×10^7
Scheme 2. Immobilized glucose oxidase. PEG + ferrocene methanol in solution	1.2×10^7
Scheme 2. Immobilized glucose oxidase. PEGFc in solution	2.2×10^5
Scheme 2. Immobilized glucose oxidase. Attached PEGFc	1.5×10^6
Scheme 1. Immobilized glucose oxidase. PEGFc in solution	6×10^5
Scheme 1. Immobilized glucose oxidase. Attached PEGFc	1×10^4

[a] In a pH 8.0 phosphate buffer (0.1 M ionic strength) at 25 °C.

diffusion of the attached ferrocene to the glucose oxidase flavin is not the rate-determining step of the reaction. We are thus led to the conclusion that the role of the chains is to sterically hinder, albeit to a modest extent, the formation of the properly oriented precursor complex. We note, in this connection, from Fig. 3(a) and 3(b), that electron transfer takes place when the chains are largely extended. Indeed, at full extension, the length of the chains is *ca.* 250 Å, while electron transfer occurs when their length lies in between 135 and 225 Å. When the PEGFc chains are free to move in the solution they have the shape of random coils. On average, the ferrocenium ions are then less accessible than in extended chains. This effect may overcompensate the larger number of conformations available in solution, finally resulting in the more difficult formation of the pre-reaction complex. These differences may thus explain the lesser reactivity of the free moving as compared to the attached PEGFc chains.

The situation is quite different in this respect in the system depicted in Scheme 1. As represented in Fig. 3(a′) and 3(b′), the PEGFc chains are much less extended, when they enter the range of distances within which the reaction takes place. As a consequence, they keep much of a random coil shape in this interval. It is thus conceivable that the smaller number of conformations in the attached case as compared to the free moving case may not be compensated by a geometry that would be more appropriate to the formation of the pre-reaction complex, as it was in the preceding system. This different balance of the two effects may explain why free moving chains are more reactive than the attached chains in this case. It may also explain why the reactivity of the attached chains is higher in the Scheme 2 system than in the Scheme 1 system.

We have noted in the preceding section that the presence of large amounts of glucose or sucrose increases the apparent reactivity of the ferrocenium heads with the enzyme, the pseudo-first order rate constant $k\tilde{C}_P^{es}$ passing from 48 to 97 s^{-1}. The interaction of glucose or sucrose with the PEG chains modifies their association with water, causing a variation of the force constant, χ_{spr}. The observed effect points to a decrease of the force constant resulting in an increase of the average concentration of the ferrocenium heads at the enzyme flavins.

Conclusions

Introduction of an antibody labeled with poly(ethylene glycol) linear chains ended by a one-electron transfer head in the previously developed antigen–antibody strategies allows the attachment onto an electrode of an enzyme monolayer in which both the enzyme and the mediator are bound. As illustrated with the example of glucose oxidase and a ferrocene mediator, the enzyme preserves its full activity in such structures, which may be easily reproduced. In spite of their fixation to the structure, the mobility of the ferrocene heads is sufficient to ensure that its transport to the enzyme prosthetic group is not rate determining. As compared to simple ferrocenium ions, such as ferrocenium methanol, the decrease in reactivity of the attached mediator is modest. It is related to a slight decrease in efficiency of the molecular recognition between the enzyme and the mediator required for electron transfer to take place. Analyzing the dynamics of this system, in comparison with previous systems, was an occasion to shed further light on the recognition phenomenon. Based on variations of the electron transfer driving force and on the effect of the electric charge borne by the mediator, it may be concluded that the electron transfer step is not, in itself, rate determining. The reaction is rather controlled by the prior formation of a complex between the ferrocenium ion and the flavin required for electron transfer to occur. The efficiency of this step is affected by steric hindrance and the various observations made with free-moving and attached ferrocene-ended poly(ethylene glycol) chains may be rationalized by the interplay of factors controlling their distribution and shape.

This enzyme monolayer integrated system is a good starting point for the step-by-step construction of spatially ordered multilayered assemblies with strong catalytic efficiencies. In view of the present results, fast responding systems are expected both in terms of electron transport and electron transfer between the mediator and the enzyme. The spatial order resulting from the step-by-step construction should allow a much more precise analysis of electron transport and electron transfer than in conventional assemblies of redox centers. Mastering both the construction and the functioning of such systems should be helpful in the design of more complex systems, integrating additional functionalities electrically controlled by means of their electron transport/transfer connection to the electrode surface.

References

1 A. P. F. Turner, I. Karube and G. S. Wilson, in *Biosensors*, Oxford University Press, Oxford, 1987.
2 *Biosensors, Principles and Applications*, ed. L. J. Blum and P. R. Coulet, Marcel Dekker, New York, 1991.
3 H. Simon, J. Bader, H. Gunther, S. Neumann and J. Thanos, *Angew. Chem., Int. Engl. Ed.*, 1985, **24**, 539.
4 S. C. Laane, W. Pronk, M. Franssen and C. Veeger, *Enzyme Microb. Technol.*, 1984, **6**, 165.
5 C. Bourdillon, R. Lortie and J. M. Laval, *Biotechnol. Bioeng.*, 1988, **31**, 553.
6 M. Frede and E. Steckhan, *Tetrahedron Lett.*, 1991, **32**, 5063.
7 J.-M. Savéant and E. Vianello, in *Advances in Polarography*, ed. I. S. Longmuir, Pergamon Press, London, 1960, vol. 1, p. 367–374.
8 C. P. Andrieux and J.-M. Savéant, in *Electrochemical Reactions in Investigation of Rates and Mechanisms of Reactions, Techniques of Chemistry*, ed. C. F. Bernasconi, Wiley, New York, 1986; vol. VI/4E, part 2, p. 305–390.
9 C. P. Andrieux, P. Hapiot and J.-M. Savéant, *Chem. Rev.*, 1990, **90**, 723.
10 A. Heller, *Acc. Chem. Res.*, 1990, **23**, 128.
11 T. J. Ohara, M. S. Vreeke, F. Battaglini and A. Heller, *Electroanalysis*, 1993, **5**, 825.
12 S. Cosnier, *Electroanalysis*, 1997, **9**, 894.
13 W. Muller, H. Ringsdorf, E. Rump, G. Wilburg, X. Zhang, L. Angermaier, W. Knoll, M. Liley and J. Spinke, *Science*, 1993, **262**, 1706.
14 J. Spinke, M. Liley, H.-J.Guder, L. Angermaier and W. Knoll, *Langmuir*, 1993, **9**, 1821.
15 Y. Lvov, K. Ariga, I. Ichinose and T. Kunitake, *J. Am. Chem. Soc.*, 1995, **117**, 6117.
16 P. N. Bartlett and P. R. Birkin, *Anal. Chem.*, 1993, **65**, 1118.
17 P. N. Bartlett and P. R. Birkin, *Anal. Chem.*, 1994, **66**, 1552.
18 J. Hodak, R. Etchenique, E. Calvo, K. Singhal and P. N. Bartlett, *Langmuir*, 1997, **13**, 2708.
19 C. Bourdillon, C. Demaille, J. Guéris, J. Moiroux and J.-M. Savéant, *J. Am. Chem. Soc.*, 1993, **115**, 12264.
20 C. Bourdillon, C. Demaille, J. Moiroux and J.-M. Savéant, *J. Am. Chem. Soc.*, 1994, **116**, 10328.
21 C. Bourdillon, C. Demaille, J. Moiroux and J.-M. Savéant, *J. Am. Chem. Soc.*, 1995, **117**, 11499.
22 C. Bourdillon, C. Demaille, J. Moiroux and J.-M. Savéant, *Acc. Chem. Res.*, 1996, **29**, 529.
23 C. Demaille, J. Moiroux, J.-M. Savéant and C. Bourdillon, in *Protein Architecture: Interfacing Molecular Assemblies and Immobilization Biotechnology*, ed. H. Möhwald and Y. Lvov, Marcel Dekker, New York, 1999, p. 311.
24 P. Pantano, T. H. Morton and W. G. Kuhr, *J. Am. Chem. Soc.*, 1991, **113**, 1832.
25 P. Pantano and W. G. Kuhr, *Anal. Chem.*, 1993, **65**, 623.
26 N. Dontha, W. B. Nowall and W. G. Kuhr, *Anal. Chem.*, 1997, **69**, 2619.
27 Z. Liu, Y. Wang, S. P. Kounaves and E. J. Brush, *Anal. Chem.*, 1995, **67**, 1679.
28 N. Anicet, C. Bourdillon, J. Moiroux and J.-M. Savéant, *J. Phys. Chem. B*, 1998, **102**, 9844.
29 N. Anicet, A. Anne, J. Moiroux and J.-M. Savéant, *J. Am. Chem. Soc.*, 1998, **120**, 7115.
30 N. Anicet, C. Bourdillon, J. Moiroux and J.-M. Savéant, *Langmuir*, 1999, **15**, 6527.
31 A. Anne and J. Moiroux, *Macromolecules*, 1999, **32**, 5829.
32 A. Anne, C. Demaille and J. Moiroux, *J. Am. Chem. Soc.*, 1999, **121**, 10379.
33 M. K. Weibel and H. J. Bright, *J. Biol. Chem.*, 1971, **246**, 2734.
34 J. C. Lee and L. L. Y. Lee, *J. Biol. Chem.*, 1981, **256**, 625.
35 T. Arakawa and S. N. Timasheff, *Biochemistry*, 1985, **24**, 6756.
36 J. C. Lee and L. L. Y. Lee, *Biochemistry*, 1987, **26**, 7813.
37 W. N. Ye, D. Combes and P. Monsan, *Enzyme Micob. Technol.*, 1988, **10**, 498.
38 C. Bourdillon, C. Demaille, J. Moiroux and J.-M. Savéant, *J. Am. Chem. Soc.*, 1993, **115**, 2.
39 P. Alzari, N. Anicet, C. Bourdillon, J. Moiroux and J.-M. Savéant, *J. Am. Chem. Soc.*, 1996, **118**, 6788.
40 H. J. Hetch, H. M. Kalisz, J. Hendle, R. D. Schmid and D. J. Schomburg, *J. Mol. Biol.*, 1993, **229**, 153.
41 G. Wohlfarht, S. Witt, J. Hendle, D. J. Schomburg, H. M. Kalisz and H. J. Hetch, *Acta Crystallogr., Sect. D*, 1999, **55**, 969.
42 S. Marx-Tibbon, E. Katz and I. Willner, *J. Am. Chem. Soc.*, 1995, **117**, 9925.
43 P. Flory, in *Principles of Polymer Chemistry*, Cornell University Press, Itheca, NY, 1986, ch. V.